

# A gait analysis data collection and reduction technique \*

Roy B. Davis III, Sylvia Öunpuu, Dennis Tyburski  
and James R. Gage

*Newington Children's Hospital, Newington, USA*

## Abstract

Davis, R.B., III, S. Öunpuu, D. Tyburski and J.R. Gage, 1991. A gait analysis data collection and reduction technique. *Human Movement Science* 10, 575–587.

The clinical objective of the gait analysis laboratory, developed by United Technologies Corporation (Hartford, CT, USA) in 1980, at the Newington Children's Hospital is to provide quantified assessments of human locomotion which assist in the orthopaedic management of various pediatric gait pathologies. The motion measurement system utilizes a video-based data collection strategy similar to commercially available systems for motion data collection. Anatomically aligned, passive, retroreflective markers placed on the subject are illuminated, detected, and stored in dedicated camera hardware while data are acquired from force platforms and EMG transducers. Three-dimensional marker position information is used to determine: (i) the orientation of segmentally-embedded coordinate systems, (ii) instantaneous joint center locations, and (iii) joint angles. Joint kinetics, i.e., moments and powers, may also be computed if valid force plate data are collected.

## Introduction

Gait analysis is the systematic measurement, description, and assessment of those quantities thought to characterize human locomotion. Through gait analysis, kinematic and kinetic data are acquired and analyzed to provide information which describes fundamental gait characteristics and which is ultimately interpreted by the clinician(s) to form an assessment. The clinical application of gait analysis allows the clinician to evaluate quantitatively the degree to which an individual's

\* Requests for reprints should be sent to R.B. Davis, Gait Analysis Laboratory, Newington Children's Hospital, 181 East Cedar Street, Newington, CT 06111, USA.

gait has been affected by an already diagnosed disorder, that is, clinical gait analysis is presently an evaluation tool and not a diagnostic tool (Brand and Crowninshield 1981). This perspective may change with the appropriate application of expert systems-based pattern recognition strategies, or through the production of different, perhaps more patient specific, gait information for clinical assessment. Perhaps for gait analysis to become more useful diagnostically, 'it must overcome the stage where it supplies information about how man walks and begin to answer the relevant whys' (Cappozzo 1983). Examples of the current utilization of gait analysis clinically include: (i) the assessment of cerebral palsy locomotion to aid in the determination of appropriate surgical or orthotic intervention (Gage 1983), (ii) the examination of the progression of neuromuscular disorders such as Parkinson's or muscular dystrophy (Murray et al. 1978), and (iii) the quantification of the effects of orthopaedic surgery through the comparison of pre- and post-operative patterns (Gage et al. 1984).

The technology available for clinical gait assessment has been limited, until relatively recently, to a variety of measurement devices attached directly to the subject, such as footswitches (Blanc and Vadi 1981) or electrogoniometers (Chao 1980). The use of cinematographic film methods (Sutherland and Hagy 1972) for the measurement of limb segment displacements is well established as a research tool, however, this highly labor intensive technique presents limitations in the clinical setting. More complex (and more expensive) data collection techniques employ optical tracking systems to quantify the displacement of markers placed on body segments. The Newington Children's Hospital (NCH) gait analysis system employs this video-based data collection strategy which is similar to commercially available systems for motion data collection, for example, *Vicon* (Oxford Metrics, Limited, Oxford, England) and *ExpertVision* (Motion Analysis, Incorporated, Santa Rosa, CA, USA).

This paper describes the clinical gait analysis system that is currently in use at the Newington Children's Hospital. The clinical objectives of this laboratory are to provide quantified assessments of human locomotion which assist in the orthopaedic management of pediatric gait pathologies. Although a brief hardware description is provided, the focus of this presentation is an outline of the clinical testing protocol that is used for data collection and a description of the algorithms used to reduce the gait data.

## **Laboratory and system description**

The Gait Analysis Laboratory at NCH was developed by United Technologies Corporation (Hartford, CT, USA) in 1980. Over 1,200 patients have been seen in the laboratory in the past nine years with a current referral rate of approximately eight patients per week. The motion measurement system used in this laboratory employs three CCD (charge coupled device) cameras (Model 4815, Cohu Corporation, San Diego, CA, USA) with frame-transfer capability and 754 by 488 active elements configured in a non-interlaced mode to acquire data at either 30 or 60 frames per second. Anatomically aligned, retroreflective markers placed on the subject (described below) are illuminated by pulses of infrared light. Dedicated camera hardware performs marker detection and preprocessing before storage in the camera semiconductor memory once they have been triggered by the data collection computer (PDP-11/44, Digital Electronics Corporation (DEC), Nashua, NH, USA). Simultaneous high speed data acquisition of force platform (Advanced Mechanical Technology, Incorporated, Newton, MA, USA) signals and/or electromyographic signals (Biosentry, Incorporated, Torrance, CA, USA) are accomplished by the PDP-11/44. After collection, the data are transferred via Ethernet to a DEC MICROVAX 3600 for processing.

## **Data collection protocol**

A standard clinical patient testing protocol has been developed at NCH which is used for routine data collection. The steps associated with this process are described and rationalized as follows:

(1) *Videotaping prior to examination.* Videotape archiving of the patient's gait is advisable for a number of reasons. For example, the subject is allowed to use assistive devices such as walkers, which may not be allowed during the test because of marker obstruction. Furthermore, a videotape record allows a close examination of abnormal foot dynamics such as dynamic varus/valgus and mid-foot abnormalities. A videotape of the subject, not encumbered in any way by markers, provides the clinician with an overall or 'global' view of the subject and additional documentation for later presentation, discussion, and teach-

ing. A videotape of the subject is also occasionally useful as a quality control mechanism.

(2) *Physical evaluation and measurement.* An examination of the patient provides an assessment of the muscle strength and tone, joint range of motion, bony abnormalities, and fixed muscular contractures. In addition, anthropometric measurements are made at this time which include the subject's height, weight, and leg lengths. Data are also collected which are used in the estimation of the joint center locations, i.e., the knee and ankle widths (as seen in the coronal plane of the limb), the distance between right and left pelvic anterior superior iliac

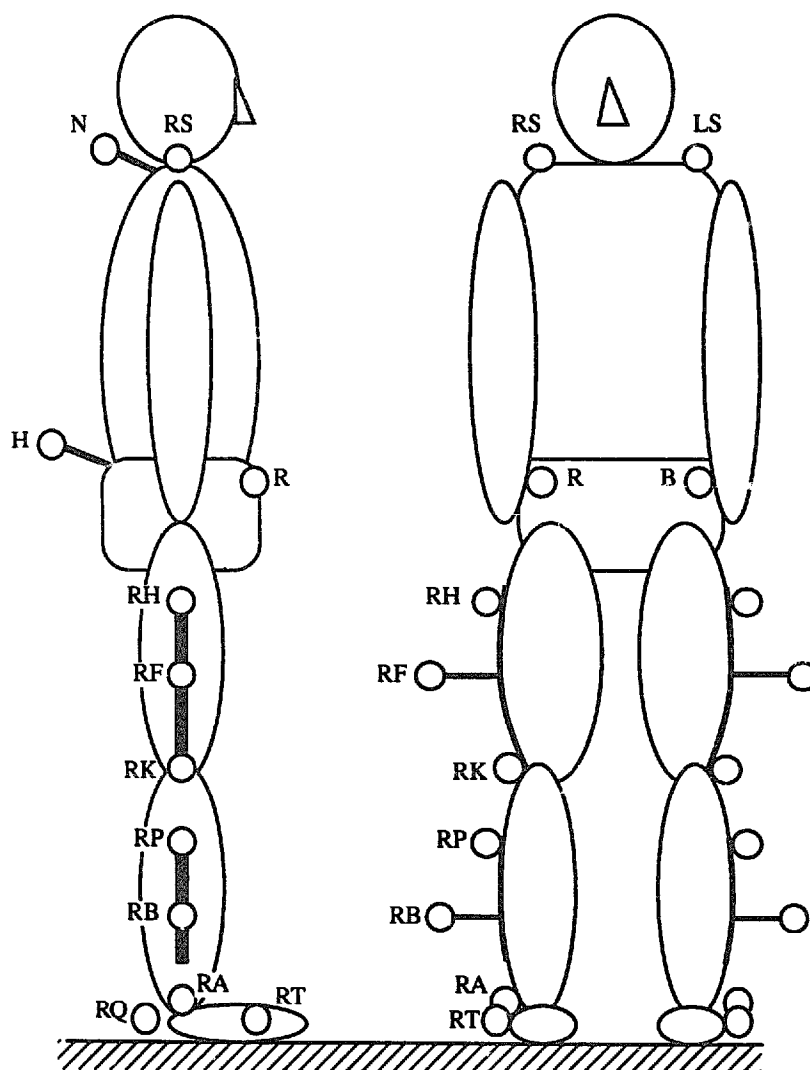


Fig. 1. Marker configuration developed and employed at the Newington Children's Hospital.

spine (ASIS), and the vertical distance in the sagittal plane of the supine subject between the ASIS and the greater trochanter (with the femur rotated such that the greater trochanter is oriented as lateral as possible).

(3) *Marker placement.* The reader is referred to the description of this process provided below.

(4) *Static offset measurement.* While the subject stands in the measurement volume of the motion camera system, marker data are collected to establish the location(s) of each lower extremity joint center relative to the associated segmentally-fixed coordinate system. This data reduction procedure is described further below.

(5) *Motion test.* Data from a minimum of three barefoot walks (with at least one full left and right gait cycle each walk) are collected. Data from an orthotic-assisted walk is also obtained if appropriate.

(6) *Electromyographic (EMG) assessment.* Surface and/or finewire electrodes for EMG measurement are placed on the subject following a standard placement guideline provided by Delagi et al. (1985). Muscles currently evaluated via EMG include, but are not limited to, the quadriceps, hamstrings, triceps surae (gastroc/soleus), anterior tibialis (finewire, depending on size), and posterior tibialis (finewire). Multiple strides of EMG data are collected on a strip chart recorder to assess the variability of each signal relative to the particular cycle selected for computer-based data acquisition. Foot contact and foot off are identified via videotape analysis.

### **Marker configuration and alignment**

The retroreflective marker set used at the NCH Gait Lab is shown in fig. 1. This marker set has evolved over the past nine years and represents the minimal configuration for a *three-dimensional, bilateral* analysis of gait. The markers are placed on the subject according to the following specifications:

*Pelvis.* The 'R' and 'B' markers are placed over the right and left ASIS, respectively. The base of the sacral 'H' wand marker is positioned over the subject's posterior superior iliac spine (PSIS) with the wand angle adjusted such that the H marker lies in the plane formed by the subject's right and left ASIS and PSIS.

*Thigh.* The subject's right medial and lateral epicondyles are palpated and an alignment fixture is positioned over the epicondyles such that

the fixture is in line with the epicondular axis. The right thigh marker set, i.e., the RK, RF, and RH markers, is placed on the subject such that the identified epicondular axis lies in the plane formed by these three markers. Also, the RK marker is positioned along the epicondular axis and the marker plane is oriented so that the longitudinal axis of the thigh lies in the plane formed by the three markers. Note that these three markers are fastened together in a relatively rigid cluster and are placed on the subject as a unit with attachment as distal as possible on the thigh in order to minimize skin motion artifact. This process is repeated for the subject's left side.

*Shank.* The right shank markers, RA, RB, and RP, are placed on the subject to form another plane in which the epicondular axis is found. That is, the intersection of properly aligned thigh and shank marker set planes is represented by the epicondular axis. The separate RA marker is placed *at the level of*, but not necessarily over (depending on the subject's tibial rotation characteristics), the lateral malleolus. The shank marker plane is oriented so that the longitudinal axis of the shank lies in this plane. Again, the cluster of markers is placed on the limb segment as distal as possible in order to reduce motion artifact. This procedure is duplicated for the subject's left side.

*Foot.* The right toe marker (RT) is placed on the lateral aspect of the foot at the fifth metatarsal head. A heel marker (RQ) is used only during the static offset measurement and is positioned so that the heel-toe marker vector is parallel to (but offset from) the sole of the foot and aligned with the foot progression line, i.e., the line from the ankle center to the space between the second and third metatarsal heads. This process is repeated for the left side.

*Trunk.* The shoulder markers (RS and LS) and cervical wand marker (N) are placed on the subject so that the line which passes through the sternoclavicular joint and the seventh cervical vertebrae is parallel with this marker plane. Each shoulder marker is placed mid-distance between the neck and the lateral aspect of the shoulder.

### **Kinematics data reduction protocol**

After the walk is complete and all camera information has been collected, the two-dimensional coordinates of the centroid of each

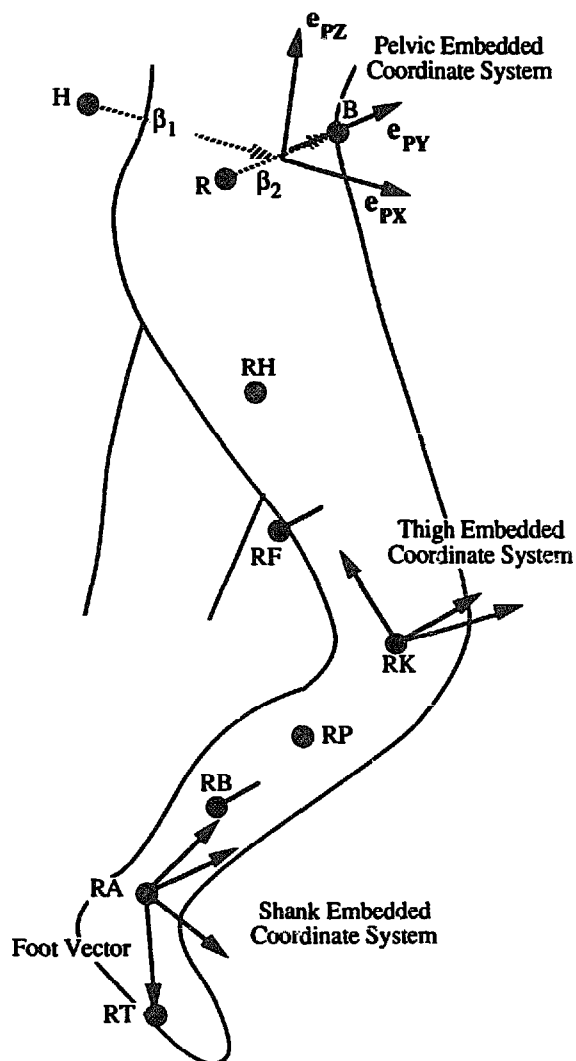


Fig. 2. Lower extremity, embedded coordinate systems used to compute the joint angles and as frames of reference for the joint moment reactions.

marker image are determined for each frame of camera data. Each marker image is then identified in two frames of motion data (for each camera or view) by the operator. In this way, the data are tracked with operator assistance. Three dimensional marker coordinates are computed stereometrically from the two dimensional camera data. The instantaneous orientation of an orthogonal, marker-based, embedded coordinate system (fig. 2) is determined for the trunk and pelvis and each thigh, shank, and foot segment. The marker-based embedded coordinate systems for the thigh, shank, and foot are then realigned with the instantaneous, joint center-based, embedded coordinate sys-

tems. The angular offset values used in this realignment process are computed from the standing data collected prior to the motion test. Finally, three dimensional limb segment rotation angles are calculated from the embedded coordinate system information. The sections that follow describe the details associated with the determination of the embedded coordinate systems, the joint center locations, and the joint angles.

### *Embedded coordinate systems determination*

An embedded or body-fixed coordinate system may be determined for any body segment (assumed to be rigid) that has at least three non-colinear markers attached to it. For example, the pelvic coordinate system is constructed from the three-dimensional location vectors of the three pelvic markers,  $R$ ,  $B$ , and  $H$  in the following manner. First, vectors  $\beta_1$  and  $\beta_2$  (fig. 2) are defined,

$$\beta_1 = 0.5(R + B) - H. \quad (1)$$

$$\beta_2 = B - R. \quad (2)$$

$\beta_2$  is then normalized to define unit vector  $e_{PY}$ . The vector  $\beta_3$  is then computed with a Gram-Schmidt orthogonalization procedure,

$$\beta_3 = \beta_1 - (\beta_1 \cdot e_{PY})e_{PY}. \quad (3)$$

$\beta_3$  is normalized to become unit vector  $e_{PX}$ .

Finally, unit vector  $e_{PZ}$  is computed from the vector cross product of  $e_{PX}$  and  $e_{PY}$ . A similar process is repeated for each of the body segment embedded coordinate systems, e.g., the trunk, thigh, and shank.

### *Joint center determination*

The location of hip, knee, and ankle joint centers are calculated relative to the associated embedded coordinate system origin, i.e., (i) the hip center location relative to the origin of the pelvic embedded coordinate system (located midway between ASIS markers) in pelvic coordinates, (ii) the knee center location relative to the origin of the marker-based thigh embedded coordinate system (located at knee



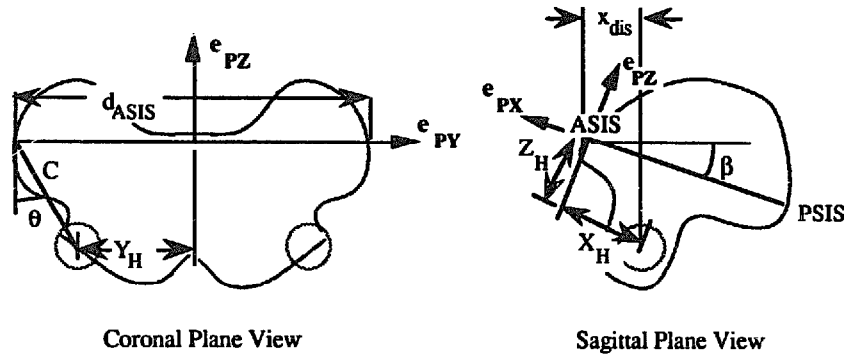


Fig. 3. Hip joint centering geometry.

marker) in thigh coordinates, and (iii) the ankle center location relative to the origin of the marker-based shank embedded coordinate system (located at ankle marker) in shank coordinates.

The basis for the hip joint centering algorithm is shown in fig. 3. This model was developed at NCH in 1981 through the radiographic examination of 25 hip studies. Particular mean values, e.g.,  $\theta$  and  $\beta$ , and relationships, such as  $C$  as a function of leg length,  $L_{\text{leg}}$  (in meters), were produced for the model through that investigation. Specifically,  $\theta$  and  $\beta$  were found to be  $28.4 (\pm 6.6)$  and  $18 (\pm 4)$  degrees, respectively, while  $C$  (in meters) may be predicted through linear regression as,

$$C = 0.115L_{\text{leg}} - 0.0153, \quad (4)$$

with an  $R$ -square correlation coefficient of 0.90. With this, the location (in meters) of the hip joint center *in pelvic coordinates* relative to the origin of the pelvic embedded coordinate system is defined as

$$X_H = [-x_{\text{dis}} - r_{\text{marker}}] \cos(\beta) + C \cos(\theta) \sin(\beta), \quad (5)$$

$$Y_H = S \left[ C \sin(\theta) - \frac{d_{\text{ASIS}}}{2} \right], \quad (6)$$

$$Z_H = [-x_{\text{dis}} - r_{\text{marker}}] \sin(\beta) - C \cos(\theta) \cos(\beta), \quad (7)$$

where:

$d_{\text{ASIS}}$  = ASIS-to-ASIS distance (in meters), measured during the clinical examination,

$x_{\text{dis}}$  = anterior/posterior component of the ASIS/hip center distance (in meters) in the sagittal plane of the pelvis and measured during the clinical examination,

$r_{\text{marker}}$  = marker radius (in meters), and

$S$  = +1 for the right side, and -1 for the left side.

The knee center location is calculated based on the coronal plane knee width measurement,  $w_{\text{knee}}$  (in meters), obtained during the patient examination, that is, the location (in meters) of the knee joint center *in thigh coordinates and relative to the lateral knee marker* is

$$X_K = 0. \quad (8)$$

$$Y_K = S(r_{\text{marker}} + 0.5 w_{\text{knee}}). \quad (9)$$

$$Z_K = 0. \quad (10)$$

The location of the ankle center employs the same strategy that is used for the knee center location.

#### *Limb rotation or joint angle determination*

The limb rotation algorithm is based on the determination of Euler angles (Greenwood 1965; Kadaba et al. 1990) with an  $y$ - $x$ - $z$  axis (fig. 2) rotation sequence. The transformation matrix which defines the orientation of a particular set of coordinate axes, e.g., the distal set  $\{e^D\}$ , relative to a reference set of coordinate axes, e.g., the proximal set  $\{e^P\}$ , is developed and employed to yield the joint angles,  $\theta_y$ ,  $\theta_x$  and  $\theta_z$ . These joint angles correspond to flexion/extension, adduction/abduction, and internal/external rotation, respectively, and are computed from the following relationships:

$$\theta_y = \sin^{-1} \left[ \frac{e_z^D \cdot e_x^P}{\cos(\theta_x)} \right]. \quad (11)$$

$$\theta_x = -\sin^{-1} [e_z^D \cdot e_y^P]. \quad (12)$$

$$\theta_z = \sin^{-1} \left[ \frac{e_x^D \cdot e_y^P}{\cos(\theta_x)} \right]. \quad (13)$$

The joint rotation angles that are routinely determined clinically are trunk and pelvic obliquity-tilt-rotation, hip ad/abduction-flexion/extension-rotation, knee flexion/extension, ankle plantar/dorsi-flexion, and foot rotation. Note that the trunk and pelvic angles are absolute angles, i.e., referenced to the inertially fixed laboratory coordinate system. The hip, knee, and ankle angles are all relative angles, e.g., the three hip angles describe the orientation of the thigh with respect to the pelvis. The foot rotation angle is an absolute angle, referenced to the laboratory, which indicates the position of the subject's foot with respect to the direction of progression. The knee ad/abduction and rotation angles are not utilized clinically because of the poor signal-to-noise ratio associated with these data.

### Kinetics data reduction protocol

The net 3D joint moments at the hip, knee, and ankle are computed via Newtonian mechanics through the application of Newton's Second Law and Euler's equations of motion (Greenwood 1965),

$$\begin{aligned} M_x &= I_{xx}\alpha_x + (I_{zz} - I_{yy})\omega_y\omega_z, \\ M_y &= I_{yy}\alpha_y + (I_{xx} - I_{zz})\omega_z\omega_x, \\ M_z &= I_{zz}\alpha_z + (I_{yy} - I_{xx})\omega_x\omega_y, \end{aligned} \tag{14}$$

where,

$M_x, M_y, M_z$  = components of the sum of the external moments (about the center of gravity of the segment) applied to the limb segment,

$\alpha_x, \alpha_y, \alpha_z$  = components of the absolute segmental angular acceleration,

$\omega_x, \omega_y, \omega_z$  = components of the absolute segmental angular velocity,

$I_{xx}, I_{yy}, I_{zz}$  = principal mass moments of inertia of the segment, and

$x, y, z$  = body-fixed coordinate axes, defined as the principal axes and located at the center of mass of the segment.

For example, the ankle reaction moment vector,  $M_A$ , and the force reaction vector,  $F_A$ , (fig. 4), may be determined with the appropriate

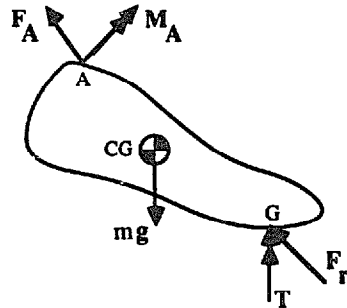


Fig. 4. Free-body diagram of the foot segment used to determine force and moment reactions at the ankle joint.

kinematic information, e.g., joint center location (point A), center of pressure coordinates (point G), and center of gravity location (point CG), as well as the external load applied to the foot, i.e., the weight of the foot,  $mg$ , the ground force reaction,  $F_r$  and the vertical torque,  $T$ . In this way, the proximal joint reactions of each segment may be determined using the distal reaction results. The joint power relative to each segmental axis is determined from the product of the joint moment vector component and the associated relative angular velocity component.

The segmental mass, mass center location and mass moment of inertia are approximated based on the relationships of Dempster et al. (1959). A weighted least squares numerical differentiation scheme is used to compute the velocities and accelerations. Moment and power resultant vectors are expressed relative to the embedded, body-fixed coordinates which are more clinically relevant.

### Refinements underway

A number of aspects of the protocol are currently under examination. For example, a new strategy has been proposed and initial experimental data collected to improve the hip joint centering algorithm. The foot model has undergone approximately eight months of intensive examination with the incorporation of subtle improvements. A number of models that predict the anthropometric characteristics of each body segment are being studied and it is anticipated that the current model will be replaced soon.

In general, the technically oriented research activities in the laboratory are focussed on the refinement of the data collection and reduction to improve the effectiveness of the information that is provided to the clinician for decision making.

## References

- Blanc, Y. and P. Vadi, 1981. An inexpensive but durable foot-switch for telemetered locomotion studies. *Journal of Biotelemetry and Patient Monitoring* 8, 240–245.
- Brand, R.A. and R.D. Crowninshield, 1981. Comment on criteria for patient evaluation tools. *Journal of Biomechanics* 14, 655.
- Cappozzo, A., 1983. Considerations on clinical gait evaluation. *Journal of Biomechanics* 16, 302.
- Chao, E.Y., 1980. Justification of triaxial goniometer for the measurement of joint rotation. *Journal of Biomechanics* 13, 989–1006.
- Delagi, E.F., A. Perotto, J. Iazzetti and D. Morrison, 1985. *Anatomic guide for the electromyographer*. Springfield, IL: Charles C. Thomas Publishers.
- Dempster, W.T., W.C. Gabel and W.J.L. Felts, 1959. The anthropometry of manual workspace for the seated subject. *American Journal of Physiological Anthropometry* 17, 289–317.
- Gage, J.R., 1983. Gait analysis for decision-making in cerebral palsy. *Bulletin of the Hospital for Joint Diseases Orthopaedic Institution* 43, 147–163.
- Gage, J.R., D. Fabian, R. Hicks and S. Tashman, 1984. Pre- and post-operative gait analysis in patients with spastic diplegia: a preliminary report. *Journal of Pediatric Orthopaedics* 4, 715–725.
- Greenwood, D.T., 1965. *Principles of dynamics*. Englewood Cliffs, NJ: Prentice-Hall.
- Kadaba, M.P., H.K. Ramakrishnan and M.E. Wooten, 1990. Measurement of lower extremity kinematics during level walking. *Journal of Orthopaedic Research* 8, 7, 849–860.
- Murray, M.P., S.B. Sepic, G.M. Gardner and W.J. Downs, 1978. Walking patterns of men with parkinsonism. *American Journal of Physical Medicine* 57, 278–294.
- Sutherland, D.H. and J.L. Hagy, 1972. Measurement of gait movements from motion picture film. *Journal of Bone and Joint Surgery* 54, 787–797.